Real-space electronic structure approach to transport in alloys

P. E. A. Turchi
Lawrence Livermore National Laboratory (L-353), P. O. Box 808, Livermore, California 94551

D. Mayou
LEPES-CNRS, 25 Avenue des Martyrs, Boîte Postale 166, F-38042 Grenoble Cedex 9, France

(Received 19 January 2001; published 27 July 2001)

We present a method for calculating dc and ac conductivities of alloys in the framework of a tight-binding description of their electronic structure. The method is entirely derived in real space, and thus requires no spatial symmetry of the underlying lattice on which the alloy is based. It also allows a calculation of conductivity in alloy cases where the chemical randomness is treated within the coherent potential approximation. Applications to simple model systems are given to illustrate the basic features, the advantages, and the range of applicability of the method.

DOI: 10.1103/PhysRevB.64.075113 PACS number(s): 71.15.−m, 71.20.Be, 72.10.Bg, 72.15.−v

I. INTRODUCTION

It has long been recognized that chemical disorder affects a majority of the physical properties of alloys, and in particular electronic transport. In many systems chemical disorder is the main source of static disorder, and can be the major source of scattering for electrons even at room temperature. In this case an estimate of transport properties can be obtained by calculating the transport coefficients within the coherent potential approximation (CPA) on the underlying periodic lattice.[1–5]

However, many systems of current interest cannot be treated along these lines. For systems with nonperiodic lattices such as quasicrystals, bulk amorphous alloys, or systems with reduced symmetries exhibiting extended defects such as interfaces or surfaces, the solution of the CPA equations (inhomogeneous CPA) is a difficult task with standard *k*-space methods. Furthermore the electron scattering can also be affected by the topology of the lattice itself. These systems require the development of methodologies capable of treating at the same time chemical disorder and the lack of structural periodicity. Under these circumstances, real-space approaches are best suited for dealing with such situations.

The purpose of this paper is to present a methodology which allows a calculation of the optical conductivity in multicomponent alloys. The chemical disorder is treated within the inhomogeneous CPA (since all sites are not necessarily equivalent), and, since the solutions of the self-consistent CPA equations are obtained with a real-space approach, no translational symmetry of the underlying lattice is required.

We aim to compute the Kubo-Greenwood formula[6] for conductivity generalized to a nonzero frequency ω. The real part of the diagonal part of the conductivity tensor in the eigenfunction representation is given by

$$\Re\sigma_{xx}(\omega)=\frac{2\pi e^2\hbar}{\Omega}\int dE\,\frac{f(E)-f(E+\hbar\omega)}{\hbar\omega}\times\langle F_{xx}(E,E+\hbar\omega)\rangle \tag{1.1}$$

where $\hbar=h/2\pi$, with h being the Planck's constant, e is the electronic charge, Ω is the volume of the system, and

$$F_{xx}(E,E')=\mathrm{Tr}[v_x\delta(E-H)v_x\delta(E'-H)], \tag{1.2}$$

where Tr stands for a sum over the sites of the lattice and the orbitals centered on these sites, and the factor 2 in Eq. (1.1) has been explicitly included to account for spin degeneracy. The $\langle\cdots\rangle$ indicates a thermodynamical average over the configurations of the alloy. As is known, the imaginary part of the conductivity is obtained from the real part by the Kramers-Krönig relation. This formula applies to static disorder only (chemical and/or structural), and the only temperature dependence is through the Fermi-Dirac distribution function $f(E)$. In Eq. (1.2), v_x is the usual velocity operator, and H is the Hamiltonian that describes the electronic structure of the system. For simplicity, here we consider the case where the so-called vertex corrections[3,5] are negligible. This amounts to rewriting $\langle F_{xx}(E,E'+\hbar\omega)\rangle$ as

$$\langle F_{xx}(E,E')\rangle\simeq\mathrm{Tr}\,v_x\langle\delta(E-H)\rangle v_x\,\langle\delta(E'-H)\rangle. \tag{1.3}$$

It is well known that this approximation is valid when scattering is isotropic, and when weak-localization contributions are also negligible, i.e., sufficiently far from the Anderson transition. In a forthcoming publication we shall show how vertex corrections can be included exactly as in the standard scattering formalism of the CPA.[5]

The paper is organized as follows. In Sec. II we describe the formalism, and in particular the CPA equations and their tight-binding representation and solution, the real-space description of conductivity, and the extension to alloys that are characterized by more general disorder. Then, in Sec. III, we present the results of a few model calculations, discuss additional properties pertaining to the expansion on which the expression for conductivity is based, and show the effect of off-diagonal disorder on electronic density of states and transport in the case of a *d*-band description of a Cu-Pd alloy. Finally, the advantages and the range of applicability of the methodology are summarized in Sec. IV, together with some concluding remarks.

II. FORMALISM

In the following we consider a system described by a tight-binding Hamiltonian H, and assume that there is chemi-

cal disorder on the various sites of the lattice with no chemical correlations between the different sites, in the spirit of the single-site mean-field CPA. In addition, the various sites of the system are not considered equivalent, and can even be associated with different local concentrations. Our aim is to evaluate the Kubo-Greenwood formula without vertex corrections within the CPA. This means that the operator $\langle \delta(E-H)\rangle$ entering Eq. (1.3) is simply replaced by the same operator calculated for the effective CPA medium, where each site n and each orbital λ carries a self-energy $\sigma_{n\lambda}(z)$.

The approach is based on the combination of a recent method for solving the CPA equations in real space,[7–9] and of a real-space method for calculating the matrix elements of the operator $\delta(E-H)$ as they appear in the Kubo-Greenwood formula.[10,11]

A. CPA equations

For the sake of clarity, let us consider a binary *A*-*B* alloy with only one *s* orbital located on each site of its underlying lattice (not necessarily periodic). The generalization to a multiband case and to multicomponent alloys is straightforward, as discussed elsewhere.[8] For now we only consider the case of diagonal disorder. The Hamiltonian H for a given configuration of the alloy is written in the form

$$H = H_0 + V, \tag{2.1}$$

where H_0 is the site off-diagonal part of the Hamiltonian that is supposed to be independent of the alloy configuration (i.e., the off-diagonal disorder is neglected), and is defined as

$$H_0 = \sum_{nm} |n\rangle t_{nm} \langle m|, \tag{2.2}$$

where t_{nm} is the hopping integral between sites n and m which, in the simplest cases examined in the following, will be equal to t, independent of the site indices, and nonzero for first-nearest-neighbor sites, and V is the random diagonal part of H given by

$$V = \sum_{n} \epsilon_n |n\rangle\langle n|, \tag{2.3}$$

where the on-site energy ϵ_n depends on the nature of the chemical species that occupies site n for the alloy configuration under consideration. These on-site energies can be defined as

$$\epsilon_n = \sum_{i} p_n^i \epsilon_n^i, \tag{2.4}$$

where i is an index that refers to the nature of the alloy species, and p_n^i is an occupation number which takes the value 0 or 1 depending on the occupancy of site n by an i species or not. In the following, we will assume that $\epsilon_n^i = \epsilon_i$ is site independent.

In accordance with the assumption behind the single-site CPA, the medium surrounding a specific site is replaced by an average medium. This medium is described by an effective Hamiltonian H^{eff} as follows: the site off-diagonal part of H^{eff} is H_0, whereas its site-diagonal part is defined by attributing a self-energy $\sigma_n(z)$ to each site n (note that the orbital index is omitted for clarity). This self-energy is calculated by imposing a self-consistency condition, which shows that the concentration-weighted average Green's function on site n is equal to the effective-medium Green's function G^{eff} on site n. This self-consistency condition reads

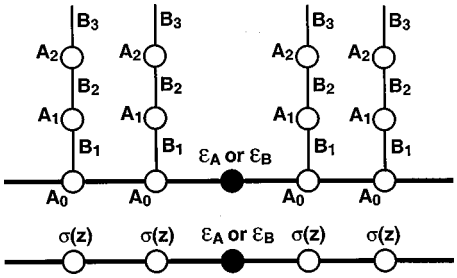

FIG. 1. Equivalent representations of the effective Hamiltonian describing chemical (diagonal) disorder within the CPA, here for a binary alloy based on an infinite linear chain (thick solid line).

$$\sum_i \frac{c_i}{z-\epsilon_i-\Delta_n(z)} = \frac{1}{z-\sigma_n(z)-\Delta_n(z)} = G_n^{\text{eff}}(z), \tag{2.5}$$

where c_i is the composition of species i, $\Delta_n(z)$ is the so-called renormalized interactor that refers to the coupling of the orbital located at site n with the surrounding effective medium,[12] and $G_n^{\text{eff}}(z)$ is the Green's function associated with the average (or effective) medium as defined within the CPA.

If all sites n are equivalent, then the self-energies $\sigma_n(z)$ and interactors $\Delta_n(z)$ are all identical, and equal to $\sigma(z)$ and $\Delta(z)$, respectively. Obviously $\Delta(z)$, that describes the coupling of an orbital with the effective medium, is a function of $\sigma(z)$, and thus Eq. (2.5) can be interpreted as a self-consistent equation for $\sigma(z)$. If the sites are not all equivalent then the self-energies $\sigma_n(z)$ depend on n, and the same is true for the interactors $\Delta_n(z)$. However, it is important to note in this case that the interactor $\Delta_n(z)$, which is determined by the environment of site n, is a function of all the self-energies $\sigma_m(z)$ for sites m different from n. Then the set of Eqs. (2.5) for all inequivalent sites n is a closed set of equations for the self-energies $\sigma_m(z)$ that can be solved in real space.[7–9]

B. Tight-binding representation of the effective CPA medium

As shown in previous papers,[7–9] there is an exact equivalence between the effective medium determined by attributing a self-energy $\sigma_n(z)$ to each site n and a standard tight-binding model where a semi-infinite chain is associated with each orbital located at each site n. This equivalence is schematically recalled in Fig. 1. When the chain parameters are properly chosen, these chains exactly simulate the effect of the self-energy. The parameters of the chain although ini-

tially unknown can be calculated starting from the beginning of the chains and moving progressively toward higher indices[7,8] with a standard recursion procedure.[13,14] This leads to expressions for the coefficients $\{A_p, B_p\}$ that are associated with each semilinear chain representation of the self-energy (see Fig. 1) in terms of the coefficients $\{a_q, b_q\}$ obtained by performing a recursion on the extended lattice. This ''dressed'' lattice is defined by a combination of the real lattice on which the alloy is based plus the semilinear chains (in principle, one per orbital) attached to each site of the lattice that represent the local self-energies. In the case of a binary alloy, these relations become[8]

$$\begin{aligned} A_0 &= \epsilon_S = c_A \epsilon_A + c_B \epsilon_B \\ B_1 &= U = \sqrt{c_A c_B}(\epsilon_A - \epsilon_B) \\ A_1 &= \epsilon_{AS} = c_B \epsilon_A + c_A \epsilon_B \\ &\cdots \\ B_p &= b_{p-1}, \quad p \geqslant 2, \\ A_p &= a_{p-1}, \quad p \geqslant 2 \end{aligned} \tag{2.6}$$

if one assumes that at the end of the first step of recursion the coefficients b_1 and a_1 are known (with $a_0 = \epsilon_A$ or ϵ_B). If one stops the procedure at a level N of recursion, the system has a finite length N along the chains but, like for clusters, it is possible to extract valuable information on the asymptotic properties of the ''exact'' infinite system provided that the cluster is large enough.[15,16] Real-space methods, and in particular the recursion method and other orthogonal polynomial methods, are well adapted to solve this kind of problem.

More precisely, if one is interested in the matrix elements of the Green's operator $\langle n|G^{\text{eff}}(z)|m\rangle$ within the CPA, then one has exactly

$$\langle n|G^{\text{eff}}(z)|m\rangle = \langle n|G^S(z)|m\rangle, \tag{2.7}$$

where $G^S(z)$ is the Green's operator associated with the tight-binding Hamiltonian H^S that describes the ''dressed'' lattice defined above. Within the CPA, the average value of the operator $\delta(E-H^{\text{eff}})$ can be expressed in terms of the Green's operator $G^{\text{eff}}(z)$ according to

$$\langle \delta(E-H^{\text{eff}})\rangle = \frac{1}{2i\pi}[G^{\text{eff}}(E-i\eta) - G^{\text{eff}}(E+i\eta)], \tag{2.8}$$

where $i\eta$ is a small positive imaginary part. Then, from this expression, one deduces

$$\langle n|\langle \delta(E-H^{\text{eff}})\rangle|m\rangle = \langle n|\delta(E-H^S)|m\rangle. \tag{2.9}$$

From the above equality, one has a way to calculate transport properties if one assumes for now no contribution from the so-called vertex corrections, since one has only to evaluate the matrix elements of the operator $\delta(E-H^{\text{eff}})$ by simply performing calculations for a tight-binding system characterized by the extended Hamiltonian H^S.

C. Real-space calculation of conductivity

A major advantage of the above approach is that it maps the CPA Hamiltonian that is energy dependent onto an energy-independent tight-binding Hamiltonian. As a consequence, all the methods that have been devised to calculate matrix elements of the Green's operator for a general tight-binding Hamiltonian are now applicable. For example, this principle was used in Ref. 8 to calculate the band energy and the effective pair interactions that describe the energy of the chemically random state of an alloy and the ordering contribution to the total energy, respectively. Here we show that it can be used efficiently to calculate the matrix elements of the off-diagonal Green's operator that are necessary for evaluating the Kubo-Greenwood formula.

Neglecting vertex corrections, we aim at computing $F_{xx}(E,E')$ which, from Eqs. (1.3) and (2.9), can be written as

$$F_{xx}(E,E') \simeq \text{Tr}_L[v_x \delta(E-H^S) v_x \delta(E'-H^S)], \tag{2.10}$$

where the notation Tr_L means a partial trace only over the sites that describe the real lattice, excluding those that make up the semilinear chains for a complete description of the tight-binding Hamiltonian H^S. With this Hamiltonian, the matrix elements of the x component of the velocity operator are defined according to

$$v_{x,nm} = \frac{i}{\hbar} H^S_{nm}(x_m - x_n) \tag{2.11}$$

where x_n is the x coordinate of the atom located at site n. Note that this expression implies that the position operator is diagonalized by the localized orbital basis functions although, in principle, this is only true in the case of an orthonormal basis of functions, as is assumed here, with zero overlap between orbitals located on neighboring sites.

The matrix element of $\delta(E-H^S)$ can be calculated by the method presented in Refs. 10 and 11. This method is based on a development in terms of orthogonal polynomials, and starts from the general expression

$$\delta(E-H) = n(E) \sum_p P_p(E) P_p(H), \tag{2.12}$$

where $n(E)$ is a reference density of states that is nonzero on the whole spectrum of the given Hamiltonian H, and the $P_p(E)$ are the orthogonal polynomials associated with the density $n(E)$. Introducing the above expression in Eq. (2.10), one obtains

$$F_{xx}(E,E') = \sum_n{}' \, \tilde{n}_n(E) n_n(E') \sum_{p,q} \tilde{P}^n_p(E) P^n_q(E') c^{xx,n}_{pq}, \tag{2.13}$$

where the sum over the site index n is indicated with a prime to mean that it is a restricted sum over only the sites of the real lattice (a restriction similar to the one that pertains to Tr_L discussed above). Also, note that the tilde on $\tilde{n}(E)$ means

that it is the density of states associated with the orthogonal polynomial $\tilde{P}$. The coefficients $c_{pq}^{xx,n}$ in the above expression are defined as

$$c_{pq}^{xx,n}=\langle n|\tilde{P}_p^n(H^S)v_xP_q^n(H^S)|n\rangle, \tag{2.14}$$

and are calculated as explained in Ref. 11, i.e.,

$$c_{pq}^{xx,n}=\tilde{}_n\{p|v_x|q\}_n, \tag{2.15}$$

where two sets of vectors have been defined according to

$$|p\}_n^{\sim}=\tilde{P}_p^n(H^S)|n\rangle=P_p^n(H^S)v_x|n\rangle,$$

$$|q\}_n=P_q^n(H^S)|n\rangle. \tag{2.16}$$

The orthogonal polynomials satisfy the three-term recurrence relation

$$HP_p^n(H)=a_p^nP_p^n(H)+b_p^nP_{p-1}^n(H)+b_{p+1}^nP_{p+1}^n(H), \tag{2.17}$$

where the coefficients a_p^n and b_p^n depend only on the chosen local density of states $n_n(E)$ at site n, and are the coefficients of the continued fraction of the Hilbert transform of $n_n(E)$. Hence one obtains similar recurrence relations for the two sets of vectors, i.e.,

$$H^S|p\}_n^{\sim}=\tilde{a}_p^n|p\}_n^{\sim}+\tilde{b}_{p-1}^n|p-1\}_n^{\sim}+\tilde{b}_p^n|p+1\}_n^{\sim}, \tag{2.18}$$

and, similarly,

$$H^S|q\}_n=a_q^n|q\}_n+b_{q-1}^n|q-1\}_n+b_q^n|q+1\}_n, \tag{2.19}$$

with the initial conditions

$$|0\}_n^{\sim}=v_x|n\rangle,$$

$$|0\}_n=|n\rangle. \tag{2.20}$$

This shows that for each inequivalent site n (and, in the general case, for each orbital) two recursions need to be performed with the starting vectors given in Eq. (2.20). Then the known values of the coefficients $(\tilde{a}_p^n,\tilde{b}_p^n)$ and (a_q^n,b_q^n) can be used to progressively calculate the vectors $|p\}_n^{\sim}$ and $|q\}_n$, respectively. Finally, one can deduce the coefficients $c_{pq}^{xx,n}$ for each lattice site n, and therefore the optical conductivity at all frequencies according to Eq. (1.1), and at any Fermi energy as described in Ref. 11 (see Appendixes A and B) without further involved calculations. In the most general case, i.e. multisite and mutiorbital, two sets of recursion per site n and per orbital λ have to be performed to evaluate one component of the conductivity tensor from the coefficients of recursion and the $c_{pq}^{xx,n\lambda}$, which are given by

$$c_{pq}^{xx,n\lambda}=\sum_{i\mu}\langle n\lambda|v_xP_p^{n\lambda}(H^S)|i\mu\rangle\langle i\mu|v_xP_q^{n\lambda}(H^S)|n\lambda\rangle$$

$$=\frac{1}{\hbar^2}\sum_{i\mu}\left(\sum_{j,\nu}(x_n-x_j)H_{nj}^{S,\lambda\nu}\langle j\nu|P_p^{n\lambda}(H^S)|i\mu\rangle\right)$$

$$\times\left(\sum_{k,\nu}(x_i-x_k)H_{ik}^{S,\mu\nu}\langle k\nu|P_q^{n\lambda}(H^S)|n\lambda\rangle\right), \tag{2.21}$$

where we made use of two closure relations and the definition of the velocity operator given by Eq. (2.11), and the summations over j and k are limited to the nearest neighbors of n and i, respectively, which involve nonzero matrix elements of the Hamiltonian.

D. Extension to alloys characterized with off-diagonal disorder

When the difference between the bandwidths of the alloy components cannot be neglected, the hopping integrals t_{nm} which enter Eq. (2.2) must depend on the site occupancy. Following the original idea of Shiba,[17] one can write a reasonable approximation for the hopping integrals as

$$t_{nm}=\alpha_nt_{nm}^0\alpha_m, \tag{2.22}$$

where t_{nm}^0 is a hopping integral that does not depend on the nature of the species located at sites n and m, and reflects the properties of the underlying ''empty'' lattice. The scalar quantity α_n, given by

$$\alpha_n=\sum_i p_n^i\alpha_i, \tag{2.23}$$

takes the value α_A (or α_B) if site n is occupied by an A (or a B) species, since p_n^i is an occupation number whose definition was given in Sec. II A. This so-called multiplicative off-diagonal disorder leads to the well-known geometrical average of a hopping integral coupling an A site to a B site according to $t_{nm}^{AB}=(t_{nm}^{AA}t_{nm}^{BB})^{1/2}$.

Within Shiba's approximation, one can show that the self-consistency condition given by Eq. (2.5) becomes[18]

$$\sum_i\frac{\tilde{c}_i}{z-\epsilon_i-\alpha_i^2\Delta_n(z)}=\frac{1}{z-\sigma_n(z)-\alpha^2\Delta_n(z)}=\tilde{G}_n(z) \tag{2.24}$$

where $\tilde{c}_i=c_i\alpha_i^2/\alpha^2$, and $\alpha^2=\Sigma_ic_i\alpha_i^2$. Note that in Eq. (2.24) we define an auxiliary Green's function $\tilde{G}$ that differs from the average CPA Green's function. Indeed, the physical projected density of states for species i located at site n is obtained from the partial Green's function according to

$$n_{n,i}(E)=-\frac{\Im}{\pi}\lim_{\eta\to0^+}\frac{1}{E+i\eta-\epsilon_i-\alpha_i^2\Delta_n(E+i\eta)}$$

$$=-\frac{\Im}{\pi}\lim_{\eta\to0^+}G_{n,i}(E+i\eta), \tag{2.25}$$

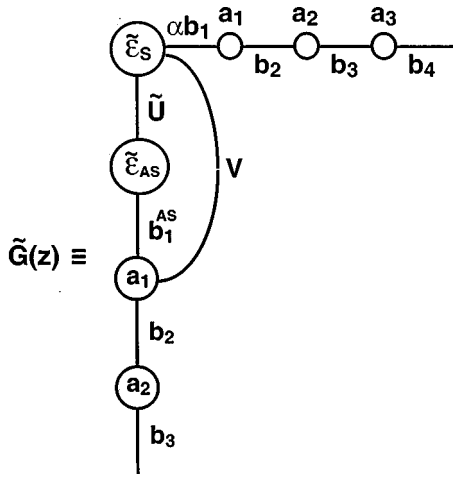

FIG. 2. Schematic representation of the auxiliary Green's function $\tilde{G}(z)$ discussed in the text in the case of a binary alloy with diagonal and off-diagonal disorder described within the CPA.

and the true average Green's function $G_n^{\mathrm{eff}}(z)$ is merely given by $G_n^{\mathrm{eff}}(z)=\Sigma_i c_i G_{n,i}(z)$, which obviously differs from $\tilde{G}_n(z)$.

It can be shown that the self-energy is now represented by a branched semilinear chain,[18] and therefore the auxiliary Green's function $\tilde{G}_n(z)$ is equivalent to the representation given in Fig. 2. The coefficients of this chain are now given by

$$\tilde{A}_0=\tilde{\epsilon}_S=\tilde{c}_A\epsilon_A+\tilde{c}_B\epsilon_B$$

$$\tilde{B}_1=\tilde{U}=\sqrt{\tilde{c}_A\tilde{c}_B}(\epsilon_A-\epsilon_B)$$

$$\tilde{A}_1=\tilde{\epsilon}_{AS}=\tilde{c}_B\epsilon_A+\tilde{c}_A\epsilon_B$$

$$\tilde{B}_2=b_1^{AS}=\alpha_A\alpha_B b_1/\alpha$$

$$V=b_1\sqrt{c_Ac_B}(\alpha_A^2-\alpha_B^2)/\alpha$$

$$\ldots$$

$$\tilde{B}_p=b_{p-1},\quad p\geqslant 3,$$

$$\tilde{A}_p=a_{p-1},\quad p\geqslant 2, \tag{2.26}$$

which are identical to the set of equations (2.6) when $\alpha_A=\alpha_B=\alpha$.

Going back to the definition of the function $F(E,E')$, given by Eq. (2.10), one has to evaluate the following quantity:

$$\mathcal{F}(z)=\mathrm{Tr}_L\langle v_x G(z) v_x G(z)\rangle. \tag{2.27}$$

Keeping in mind the definition of the restricted trace and that of the velocity operator given by Eq. (2.11), this function is proportional to

$$\left\langle \sum_{nklm}(x_n-x_k)t_{nk}\langle k|G(z)|l\rangle(x_l-x_m)t_{lm}\langle m|G(z)|n\rangle \right\rangle, \tag{2.28}$$

after insertion of two closure relations of the type $\Sigma_k|k\rangle\langle k|=I$, where I is the identity operator in Eq. (2.27). Within Shiba's approximation, this last expression is rewritten as

$$\sum_{nklm}(x_n-x_k)(x_l-x_m)\langle t_{nk}^0\alpha_k G_{kl}(z)\alpha_l t_{lm}^0\alpha_m G_{mn}(z)\alpha_n\rangle. \tag{2.29}$$

It is important to note that since the orbitals that are acted upon by the velocity operator are centered on different sites of the lattice, site occupancies become uncorrelated. This is the very same property that characterizes Shiba's approximation, since the random variables that describe off-diagonal disorder are the occupation numbers p_n^i's which are site variables, and hence local.

With the definition of $\tilde{G}$ extended to off-diagonal in-site elements given by $\langle\alpha_k G_{kl}\alpha_l\rangle=\tilde{G}_{kl}$, Eq. (2.29) becomes

$$\sum_{nklm}(x_n-x_k)(x_l-x_m)t_{nk}^0\tilde{G}_{kl}(z)t_{lm}^0\tilde{G}_{mn}(z) \tag{2.30}$$

This last expression shows that, within Shiba's approximation and the neglect of the vertex corrections, $F(E,E')$ is given in terms of the auxiliary Green's function $\tilde{G}$ and not the average Green's function G^{eff}. This makes the implementation of the recursion scheme relevant and straightforward.

III. APPLICATIONS

In this section we apply the method outlined above to a simple single-band model. For the sake of clarity we consider the case where all sites are equivalent, and show results for the densities of states, and for the dc and ac conductivities. At the end of this section we also discuss some technical aspects of the method, and present an application to the multiorbital case. In all the computations we use as a reference density of states $n(E)$ the average CPA density with the coefficients a_p and b_p calculated as explained in Refs. 7 and 8. The calculations have been performed up to $p=45$, and this ensures an excellent convergence of all the calculated quantities as will be shown.

A. Model

For the present purpose, we first consider a binary alloy based on a simple cubic lattice with one *s* orbital per site (single-band model). Since all sites are equivalent, we will consider the diagonal disorder in its simplest form, with the on-site energies taking only two values ϵ_A or ϵ_B. The hopping integral *t*, which is nonzero between nearest neighbors only, will be taken as constant throughout ($t=1/6$, so that half the bandwidth of the density of states for the pure metal *w* is equal to 1). Finally, if not specified otherwise, the concentrations of the two chemical species are equal to 0.5, and the number of exact steps of recursion is equal to 45.

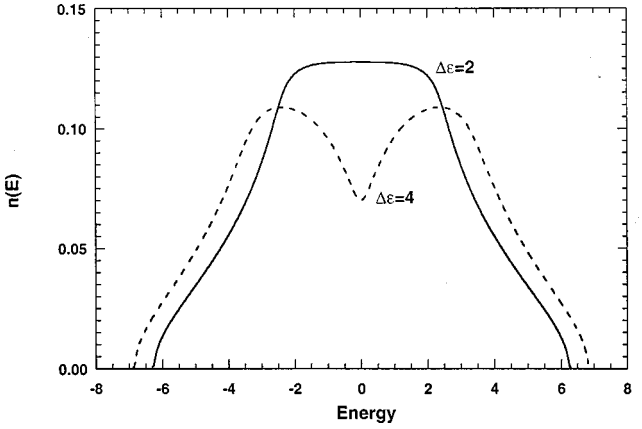

FIG. 3. Density of states for $\Delta\epsilon=2$ (solid line) and 4 (dashed line) calculated with 45 exact levels of continued fraction, for a model alloy based on a simple cubic lattice.

B. Density of states

In Fig. 3 we show the total density of states for two values of the parameter $\Delta\epsilon=\epsilon_A-\epsilon_B$ (with $\epsilon_A=-\epsilon_B$) equal to 2 and 4, which is a measure of the amplitude of the diagonal disorder. For $\Delta\epsilon=4$, the difference between the two on-site energies is sufficient to create a pseudogap in the middle of the density of states.

C. dc Conductivity

In Fig. 4 we report the normalized dc conductivity versus Fermi energy curves for $\Delta\epsilon=0.5$ and $c_A=0.1$, 0.4. These results are in excellent agreement with those of Levin *et al.*[19] (see their Fig. 6 for comparison), thus proving the validity of the real-space method for evaluating the conductivity.

Figure 5 displays the dc conductivity (i.e., conductivity at zero frequency) as a function of the Fermi energy E_F. A decrease of the conductivity in the middle of the spectrum is noticeable even for $\Delta\epsilon=2$, and becomes more pronounced as the diagonal disorder parameter increases. The results can be qualitatively interpreted as follows. The dc conductivity is

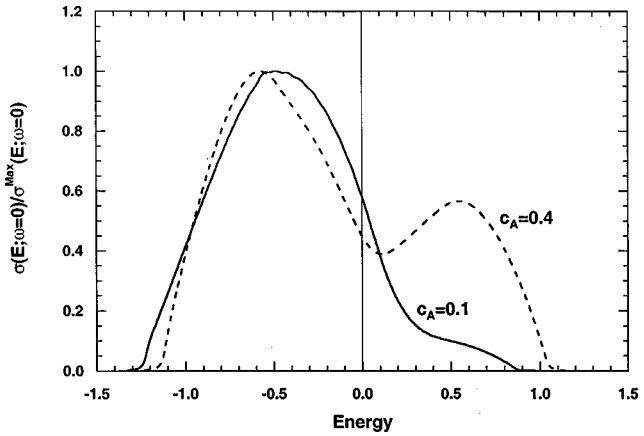

FIG. 4. Normalized dc conductivity as a function of the Fermi energy for $\Delta\epsilon=0.5$ and $c_A=0.1$ (solid curve) and 0.4 (dashed curve), calculated with 45 exact levels of continued fraction, for a model alloy based on a simple cubic lattice.

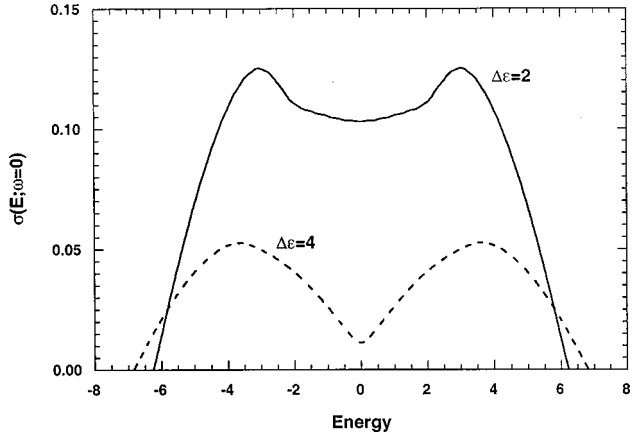

FIG. 5. dc conductivity as a function of the Fermi energy for $\Delta\epsilon=2$ (solid line) and 4 (dashed line), associated with its respective density of states displayed in Fig. 3.

equal, according to Einstein's formula, to $\sigma(E_F,\omega=0)=e^2n(E_F)D(E_F)$, where $D(E_F)$ is the so-called diffusivity defined at the Fermi energy. In the middle of the spectrum, both the densities of states $n(E_F)$ and $D(E_F)$ are reduced, thus leading to a more pronounced effect on the conductivity than on the density of states alone.

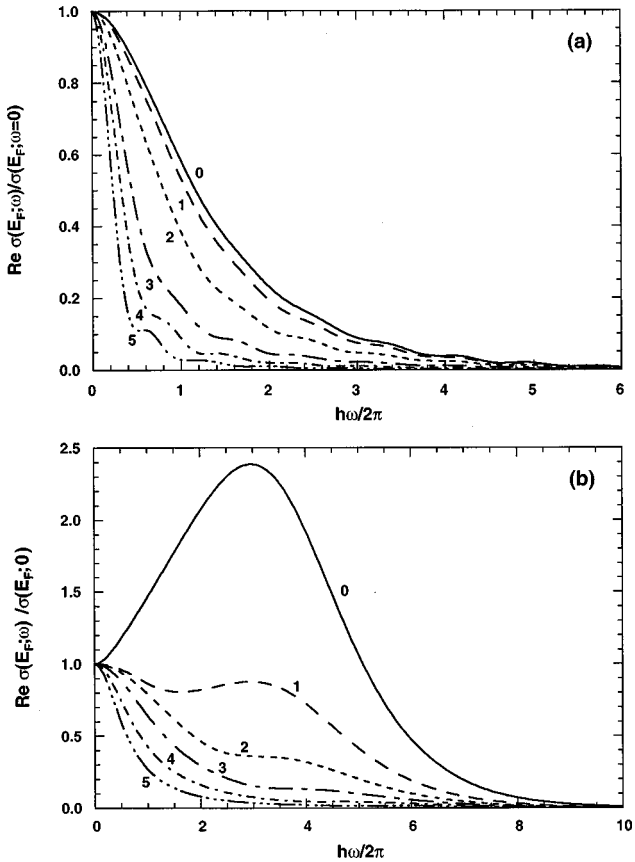

FIG. 6. ac conductivity as a function of frequency, $\hbar\omega$ for different values of the Fermi energy (0–5), and for $\Delta\epsilon=2$ (a) and 4 (b), associated with its respective density of states displayed in Fig. 3.

D. ac Conductivity

Figure 6 represents the real (dissipative) part of the ac conductivity $\sigma_{xx}(E_F,\omega)$, as a function of frequency for various values of the Fermi energy and for two diagonal disorder parameters. For $\Delta\epsilon=2$, one observes essentially a Drude-like peak (close to a Lorentzian shape with a full width at half maximum proportional to $\hbar\tau^{-1}$, where τ is the transport relaxation time) as expected for electrons in the weak scattering limit. Conversely, for $\Delta\epsilon=4$, there is a hump in the evolution of the ac conductivity with a frequency around $\hbar\omega=4$, and for E_F sufficiently close to the middle of the spectrum. This hump can be attributed to interband transitions between bands associated with species *A* and *B*, and which are separated by $\Delta\epsilon=4$. This hump will be observed if states below the middle of the spectrum are occupied, and those above it are not, which implies that the Fermi energy is not too far from the center of the spectrum.

E. Convergence of the expansion of $F_{xx}(E,E')$

It is interesting to consider some typical behavior of the two recursion vectors $|p\}_{\tilde{n}}$ and $|q\}_n$, and of the coefficients $c_{pq}^{xx,n}$ associated with a given site *n* from which the recursion process starts (in the following, when no ambiguity exists, the index *n* will be ignored, therefore implying that the lattice on which the alloy is based is periodic). These characteristics will help to understand how the expansion of $F_{xx}(E,E')$, made of a double series, converges.

First let us consider the recursion vectors $|q\}_n$. Note that in the simple example selected here, these vectors are independent of *n*, apart from a translation in real space, and are calculated by using the reference density $n(E)$ equal to the average CPA density of states shown in Fig. 3. By construction,[8] the vectors are calculated for a system where semilinear chains are attached to each site of the simple cubic lattice, and have nonzero components on the real lattice (first site of each semilinear chain) and also along the chains. As explained in Sec. II B, these chains simulate the effect of the self-energies $\sigma_n(z)$. The imaginary part of the self-energies is related to the finite lifetime τ of the states, or equivalently to the mean free path ξ of the electrons ($\xi=v\tau$, where v is a characteristic velocity for the electrons in the perfect structure). In the tight-binding representation of the CPA medium, this means that, after a distance $d>\xi$, any vector will spread essentially on the chains. Thus we expect as a rule that the recursion vectors $|p\}_{\tilde{n}}$ and $|q\}_n$ have a small vanishing weight in real space after a number of steps of the recursion process, such that they spread on a distance greater than a few times ξ. This is shown in Fig. 7, where the norm of the recursion vector $|q\}_n$ is plotted versus the number of steps of recursion for different values of the diagonal disorder parameter. Hence we conclude from this analysis that it is sufficient to have a real-space cluster of extension equal to a few ξ in order to have an accurate estimate of the conductivity.

The behavior of the recursion vectors implies that the coefficients c_{pq}^{xx} that are defined through scalar products of these vectors also decrease with *p* and *q*. Figure 8 shows the behavior of the diagonal terms c_{pp}^{xx} as a function of *p*. As

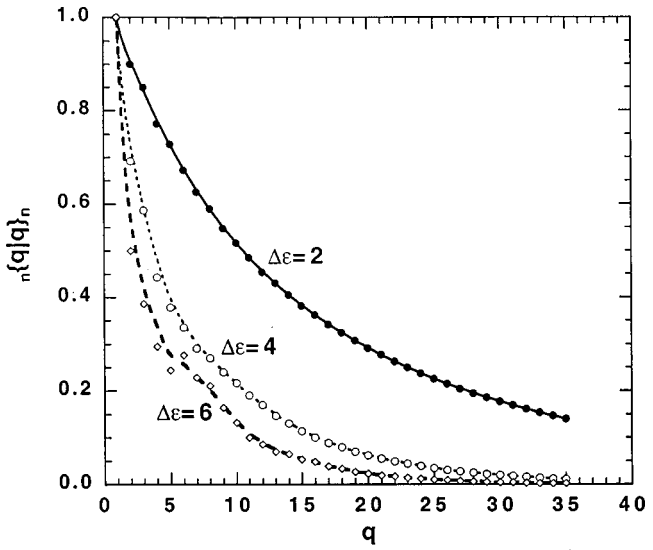

FIG. 7. Total weight of the norm of the recursion vector $|q\}_n$ in real space (i.e., on the initial state of the semilinear chains) as a function of the step *q* of the recursion procedure for the simple cubic lattice model and $\Delta\epsilon=2$, 4, and 6. Note that when disorder increases, the vectors spread more and more rapidly in the chains, as expected due to the shortening of the lifetime τ and mean free path ξ.

expected, these coefficients tend more rapidly toward zero when the diagonal disorder increases. There is also a simple sum rule that can be checked out. Indeed, by integrating Eq. (2.13) over the energy, for the integrated diffusivity one obtains

$$\int dE\, D_{xx}(E)=\int dE\,\frac{\sigma_{xx}(E)}{n(E)}=\sum_p c_{pp}^{xx}, \qquad (3.1)$$

where the orthonormality relation between the polynomials,

$$\int dE\, n(E)P_pP_q=\delta_{p,q}, \qquad (3.2)$$

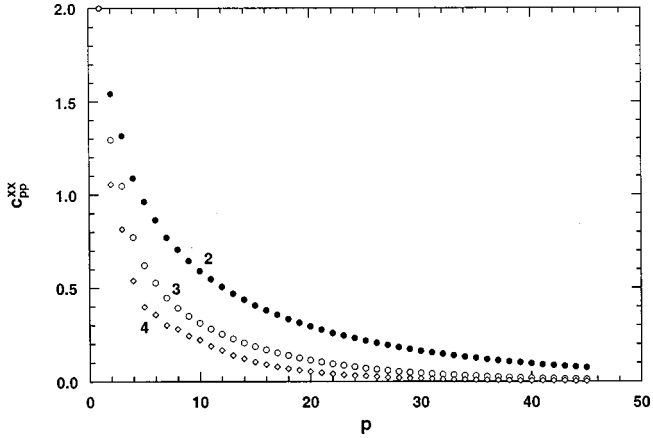

FIG. 8. Diagonal elements c_{pp}^{xx} as a function of *p* for several diagonal disorders ($\Delta\epsilon=2$, 3, and 4). The coefficients decrease rapidly with *p*, and the convergence is more rapidly achieved when the diagonal disorder increases.

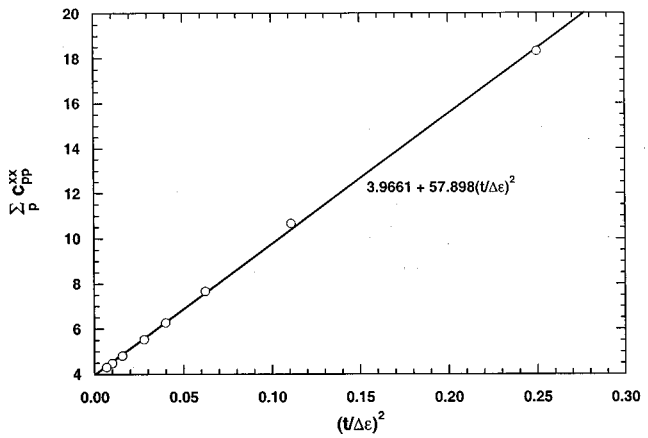

FIG. 9. Variation of $\Sigma_p c_{pp}^{xx}$ with a measure of diagonal disorder. As explained in the text, one expects that, in the weak scattering limit, this sum is proportional to $(t/\Delta\epsilon)^2$. Actually this scaling is well satisfied for a broad range of diagonal disorder $\Delta\epsilon$.

has been used, with δ being the usual Kronecker symbol. In the weak-scattering limit, the density of states tends toward the zero-disorder limit, whereas the conductivity $\sigma_{xx}(E)$, at a given Fermi energy, scales like $(t/\Delta\epsilon)^2$. Hence, in the weak-scattering limit, we expect

$$\sum_p c_{pp}^{xx} \propto \left(\frac{t}{\Delta\epsilon}\right)^2. \tag{3.3}$$

Figure 9 shows a plot of $\Sigma_p c_{pp}^{xx}$ versus $(t/\Delta\epsilon)^2$, which confirms this prediction down to a small value of $(t/\Delta\epsilon)^2$. Finally, the off-diagonal elements of c_{pq}^{xx} tend rapidly toward zero, as illustrated in Fig. 10, and more so when the diagonal disorder increases. These properties can be advantageously invoked for practical calculations to assign preasymptotic values to these coefficients without having to calculate them; in the same way, the behavior of the coefficients of the continued fraction (a_p, b_p) leads to a well-defined analytic expression for the termination of the continued fraction that expresses the one-electron Green's function.[15,16]

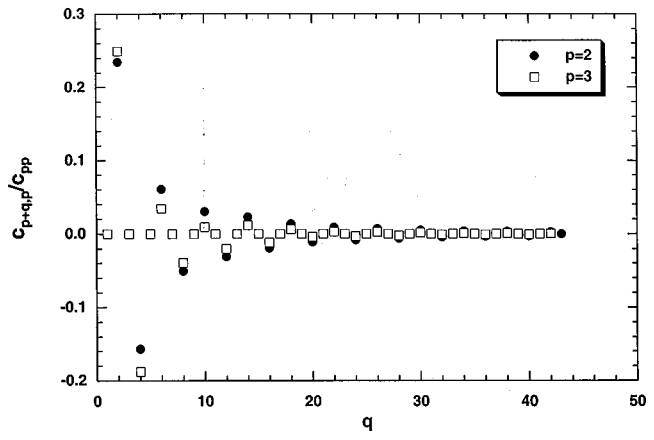

FIG. 10. Variation of typical normalized off-diagonal terms of $c_{p+q,p}^{xx}/c_{pp}$ ($p=2$ and 3) with q, showing that they tend quickly toward zero with p and q, here for $\Delta\epsilon=4$.

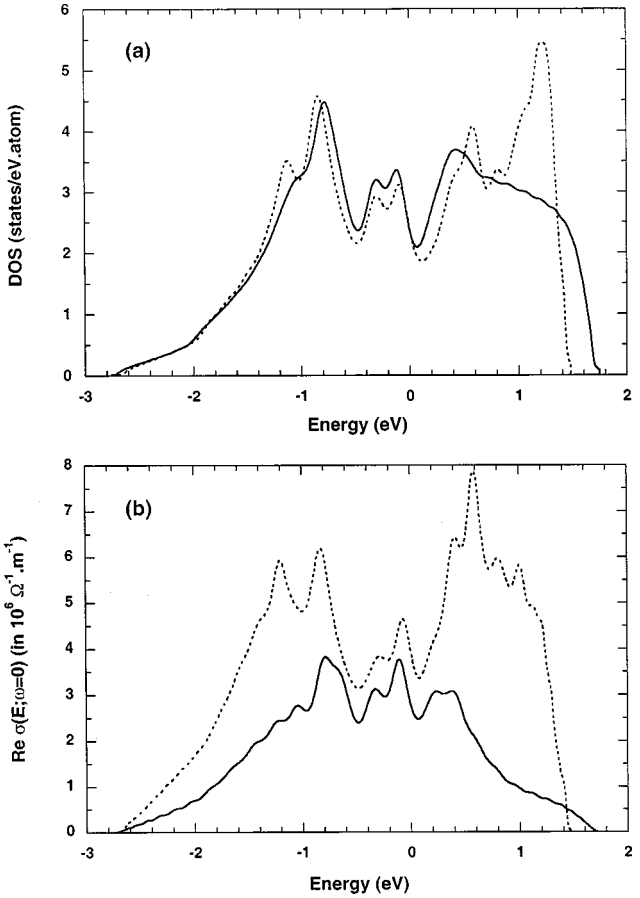

FIG. 11. Densities of states (a) and dc conductivities (b) vs energy in the case of a fcc-based $Cu_{50}Pd_{50}$ alloy described with a *d*-band model that accounts for diagonal disorder only (dotted curve), and diagonal and off-diagonal disorders (solid curve).

F. Extension to *d*-band model

In this section we show the applicability of the method to the multiorbital case and the treatment of off-diagonal disorder within the Shiba approximation. We consider the well-documented case of fcc-based Cu-Pd described here with a *d*-band tight-binding model that makes use of the Slater-Koster parametrization given in Ref. 20 for comparison purposes. That is, the nonzero hopping integrals between first nearest neighbors on the fcc lattice take the values, $dd\sigma = -16.20$ eV, $dd\pi = +8.75$ eV, and $dd\delta = 0$; the on-site energies are $\epsilon_d^{\mathrm{Cu}} = -0.15$ eV and $\epsilon_d^{\mathrm{Pd}} = 0$ eV; and the off-diagonal disorder parameters are $\alpha^2_{\mathrm{Cu}} = 0.021145$ and $\alpha^2_{\mathrm{Pd}} = 0.040194$. Figure 11(a) displays the densities of states computed within the CPA without and with off-diagonal disorder accounted for. Note that in the case of diagonal disorder only, the hopping integrals for like and unlike pairs of atoms have been multiplied by the same scalar given by the concentration weighted average of the α^2's. All calculations have been performed up to 30 levels of continued fraction. For nearby elements of the periodic table, off-diagonal disorder cannot be ignored, and accounting for this effect leads to densities of states similar to those obtained within *ab initio* approaches, such as the tight-binding linear-muffin-tin-orbital method in the present case; see Fig. 11(a), and Fig. 6

of Ref. 20 for comparison. The impact of off-diagonal disorder on transport is obviously reflected in the associated dc conductivity versus Fermi energy, as seen in Fig. 11(b). Although the tight-binding parametrization leads to the right order of magnitude for the dc conductivity, note that the *s-d* hybridization and the vertex contributions to transport should be included for a more accurate evaluation of conductivity.

IV. CONCLUSION

We have presented a methodology to calculate the optical conductivity of an alloy for which chemical randomness is treated within the CPA. In this approach calculations are performed entirely in real space, with an effective tight-binding Hamiltonian. The CPA self-energy is exactly described by attaching a semilinear chain to each orbital centered on each lattice site. Since the resulting Hamiltonian is energy independent and is of a tight-binding form, one can apply to it methods developed for solving tight-binding problems. In particular, methods based on orthogonal polynomials are applicable, and allow an efficient calculation of the conductivity expressed by the Kubo-Greenwood formula as a function of energy and frequency. As shown in this study the method is well suited for studying transport in alloys characterized by a short electron mean free path ξ, since the typical cluster size required to perform the recursions with sufficient accuracy is a few times ξ. We found that the method well reproduces departures from the Drude-like behavior of the optical conductivity caused by interband transitions, if any, as observed experimentally in some alloy cases. We have shown that the approach can be easily extended to account for off-diagonal disorder effects within Shiba's approximation.[17] Additional extensions that include a more general treatment of off-diagonal disorder such as the one proposed by Blackman *et al.*,[21] as well as of vertex corrections to transport in a way strictly equivalent to the one developed within the *T*-matrix formalism of the CPA,[3–5] are possible, and will be presented in a forthcoming publication.[18] Finally, it should be emphasized that the real-space approach described here provides a direct estimate of the projected components of the tensor of conductivity on each site of a lattice, periodic or not.

ACKNOWLEDGMENTS

This work was performed under the auspices of the U. S. Department of Energy by the University of California Lawrence Livermore National Laboratory under Contract No. W-7405-ENG-48. Partial support from NATO under Contract No. CRG 941028 is gratefully acknowledged.

[1] P. Soven, Phys. Rev. **156**, 809 (1967).
[2] B. Velický, S. Kirkpatrick, and H. Ehrenreich, Phys. Rev. **175**, 747 (1968).
[3] B. Velický, Phys. Rev. **184**, 614 (1969).
[4] E. N. Economou, in *Green's Functions in Quantum Physics*, Springer Series in Solid State Science Vol. 7 (Springer-Verlag, Berlin, 1983).
[5] W. H. Butler, Phys. Rev. B **31**, 3260 (1985).
[6] R. Kubo, J. Phys. Soc. Jpn. **12**, 570 (1985).
[7] J.-P. Julien and D. Mayou, J. Phys. I **3**, 1861 (1993).
[8] P. E. A. Turchi, D. Mayou, and J.-P. Julien, Phys. Rev. B **56**, 1726 (1997).
[9] D. Mayou, P. E. A. Turchi, S. Roche, and J.-P. Julien, in *Tight-Binding Approach to Computational Materials Science*, edited by P. G. A. Turchi, A. Gonis, and L. Colombe, MRS Symposia Proceedings No. 491 (Materials Research Society, Pittsburgh, 1998), p. 231.
[10] D. Mayou, Europhys. Lett. **6**, 549 (1988).
[11] D. Mayou and S. N. Khanna, J. Phys. I **5**, 1199 (1995).
[12] A. Gonis, in *Green Functions for Ordered and Disordered Systems*, edited by by E. van Groesen and E. M. Dejager, Studies in Mathematical Physics Vol. 4 (North-Holland, Amsterdam, 1992).
[13] R. Haydock, in *Solid State Physics*, edited by H. Ehrenreich, F. Seitz, and D. Turnbull (Academic Press, New York, 1980), Vol. 35, p. 215.
[14] *Recursion Method and its Applications*, edited by D. G. Pettifor and D. L. Weaire, Springer Series in Solid States Sciences Vol. 58 (Springer-Verlag, Berlin, 1985).
[15] P. Turchi, F. Ducastelle, and G. Tréglia, J. Phys. C **15**, 2891 (1982).
[16] G. Grosso, G. Pastori Parravicini, and A. Testa, Phys. Rev. B **32**, 627 (1985).
[17] H. Shiba, Prog. Theor. Phys. **46**, 77 (1971).
[18] J.-P. Julien, P. E. A. Turchi, and D. Mayou (unpublished).
[19] K. Levin, B. Velický, and H. Ehrenreich, Phys. Rev. B **2**, 1771 (1970).
[20] J. Kudrnovský and J. Mašek, Phys. Rev. B **31**, 6424 (1985).
[21] J. A. Blackman, D. M. Esterling, and N. F. Berk, Phys. Rev. B **4**, 2412 (1971).